

Instanton production at the LHC

Valya Khoze

IPPP Durham

with Frank Krauss & Matthias Schott [1911.09726](#) : JHEP (2020)

and Dan Milne & Michael Spannowsky [2010.02287](#) : PRD (2021)

& with Valery A Khoze, Dan Milne and Misha Ryskin

[2104.01861](#) : PRD (2021), [2111.02159](#) : PRD (2022)

QCD Instantons

Instanton-induced processes with 2 gluons in the initial state:

$$g + g \rightarrow n_g \times g + \sum_{f=1}^{N_f} (q_{Rf} + \bar{q}_{Lf})$$

\uparrow
 \vdots
 arbitrary
 (tends to be large $\sim 1/\alpha_s$)

All light flavours of quark-antiquark pairs must be present. Light \Rightarrow
 $m_f \leq 1/\rho$
 \uparrow
 \vdots
 instanton size

Can also have quark-initiated processes e.g. :

$$u_L + \bar{u}_R \rightarrow n_g \times g + \sum_{f=1}^{N_f-1} (q_{Rf} + \bar{q}_{Lf}),$$

$$u_L + d_L \rightarrow n_g \times g + u_R + d_R + \sum_{f=1}^{N_f-2} (q_{Rf} + \bar{q}_{Lf})$$

$$g + g \rightarrow n_g \times g + \sum_{f=1}^{N_f} (q_{Rf} + \bar{q}_{Lf})$$

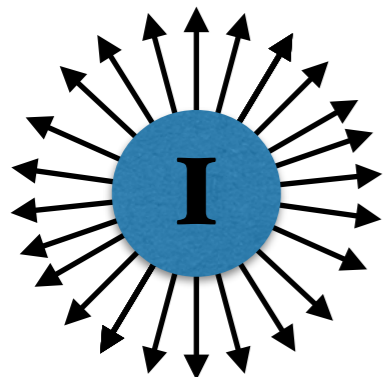
The amplitude takes the form of an integral over instanton collective coordinates.
The classical result (leading order in the instanton perturbation theory) is simply:

semiclassical suppression
(’t Hooft) factor by the instanton action

$$S_I = \frac{8\pi^2}{g^2} = \frac{2\pi}{\alpha_s(\mu_r)}$$

$$\mathcal{A}_{2 \rightarrow n_g + 2N_f} \sim \int d^4x_0 d\rho D(\rho) e^{-S_I} \left[\prod_{i=1}^{n_g+2} A_{\text{LSZ}}^{a_i \text{ inst}}(p_i, \lambda_i) \right] \left[\prod_{j=1}^{2N_f} \psi_{\text{LSZ}}^{(0)}(p_j, \lambda_j) \right]$$

- the integrand: a product of bosonic and fermionic components of the instanton field configurations
- the factorised structure implies that emission of individual particles in the final state is uncorrelated and mutually independent.



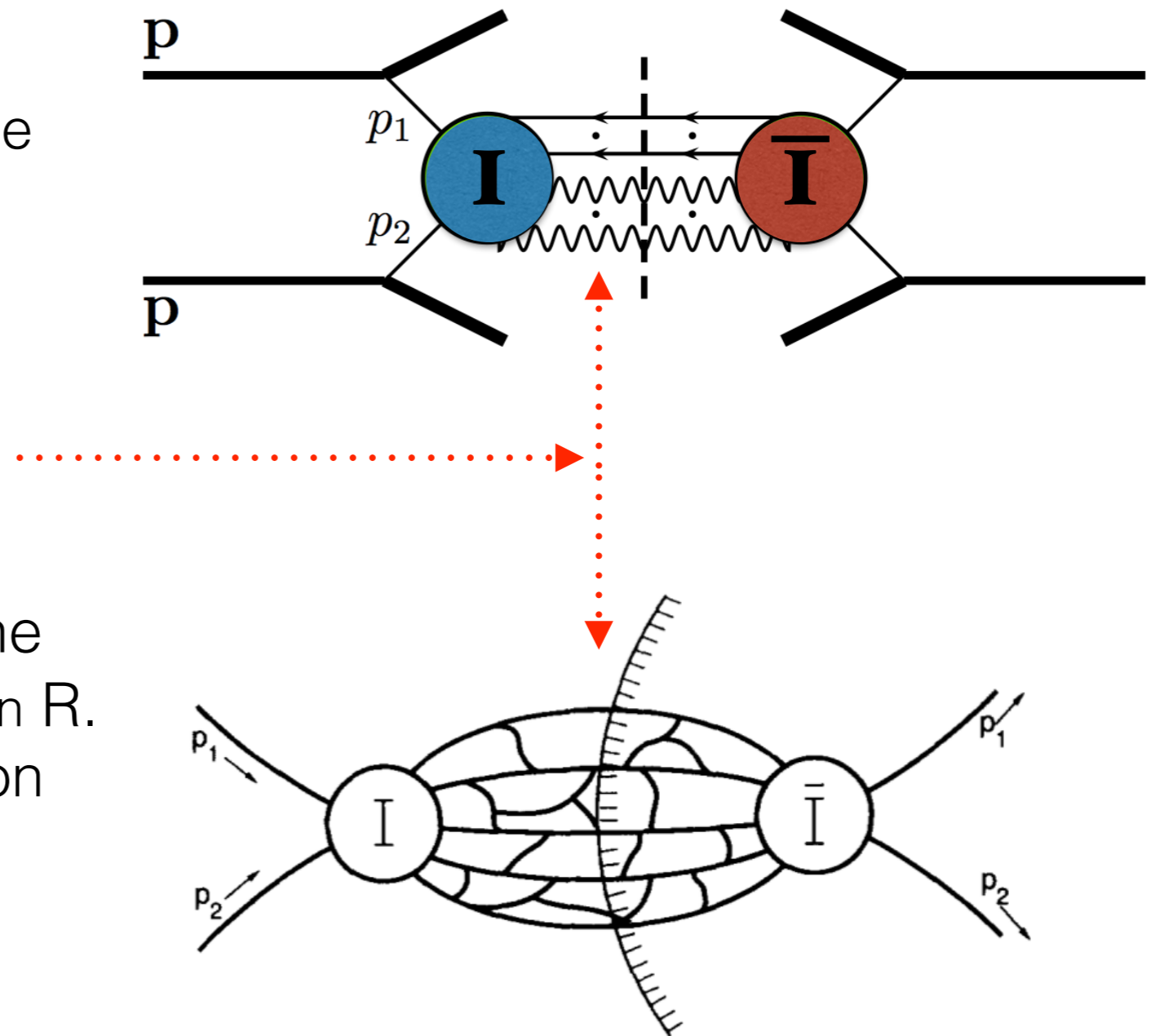
[this is correct at the LO in instanton pert. theory approximation]

LO Instanton vertex -> selection on final states at colliders with high sphericity

The Optical Theorem approach

$$\hat{\sigma}_{\text{tot}}^{\text{inst}} = \frac{1}{E^2} \text{Im} \mathcal{A}_4^{I\bar{I}}(p_1, p_2, -p_1, -p_2)$$

- Use the Optical Theorem:
- Compute **Im** part of 2->2 amplitude on an Instanton-Anti-instanton configuration
- Final states interactions effects are automatically included now
- Varying the energy E changes the Instanton-anti-Instanton separation R. At R=0 instanton and anti-instanton annihilate



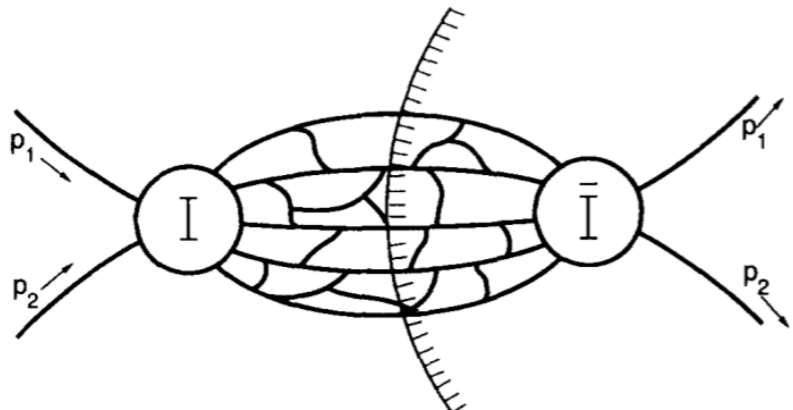
VVK & Ringwald 1991

- Instanton — anti-instanton configuration has $Q=0$; it interpolates between infinitely separated instanton—anti-instanton and the perturbative vacuum at $R=0$

(anti)-instanton sizes (anti)-instanton separation

$$\sigma_{\text{tot}}^{(\text{cl}) \text{ inst}} \simeq \frac{1}{s} \text{Im} \int_0^\infty d\rho \int_0^\infty d\bar{\rho} \int d^4 R \int d\Omega D(\rho) D(\bar{\rho}) e^{-S_{I\bar{I}}} \mathcal{K}_{\text{ferm}} \times$$

$$A_{LSZ}^{\text{inst}}(p_1) A_{LSZ}^{\text{inst}}(p_2) A_{LSZ}^{\text{inst}}(-p_1) A_{LSZ}^{\text{inst}}(-p_2),$$



$$S_{I\bar{I}}(\rho, \bar{\rho}, R) = \frac{4\pi}{\alpha_s(\mu_r)} \hat{S}$$

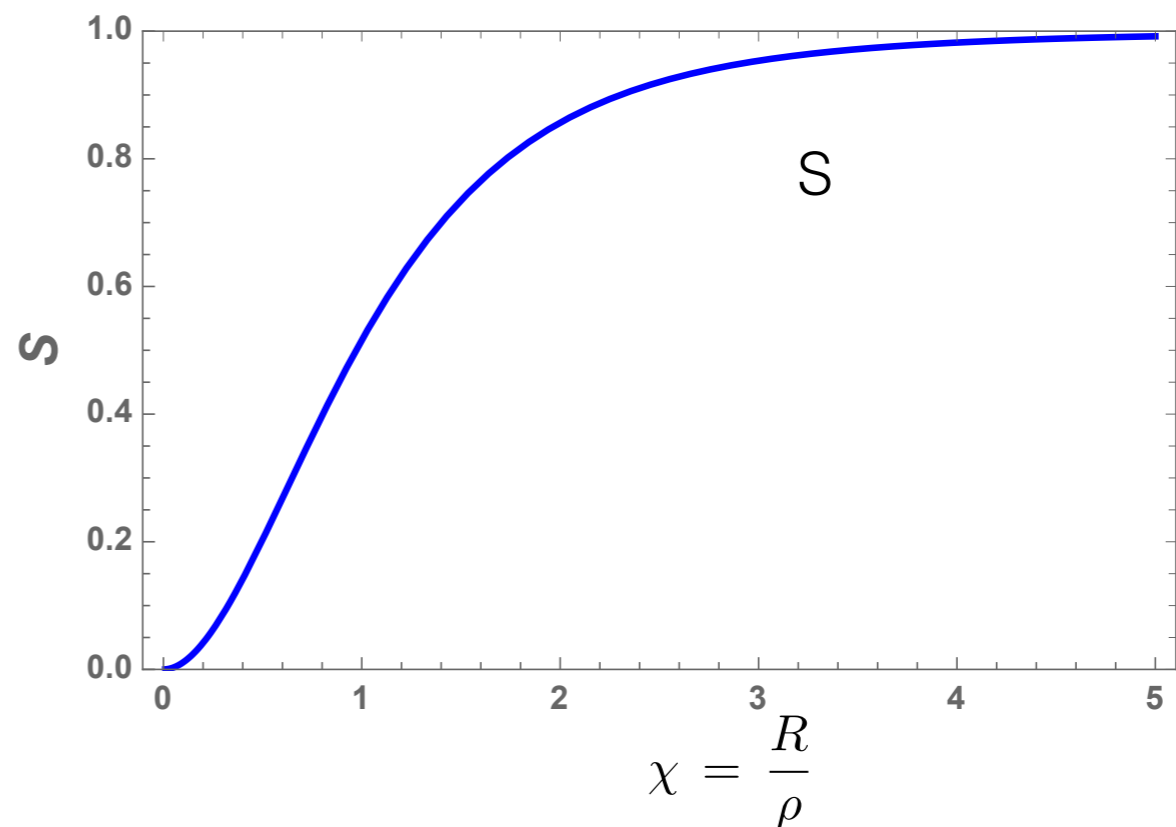
instanton-anti-instanton action
(see next slide)

- Exponential suppression is gradually reduced at lower R (Energy-dependent)
- no radiative corrs from hard initial states are yet included in this approximation

$$\begin{aligned} \sigma_{\text{tot}}^{(\text{cl}) \text{ inst}} &= \frac{1}{s} \text{Im} \mathcal{A}_4^{I\bar{I}}(p_1, p_2, -p_1, -p_2) \\ &\simeq \frac{1}{s} \text{Im} \int_0^\infty d\rho \int_0^\infty d\bar{\rho} \int d^4 R \int d\Omega D(\rho) D(\bar{\rho}) e^{-S_{I\bar{I}}} \mathcal{K}_{\text{ferm}} \times \\ &\quad A_{LSZ}^{\text{inst}}(p_1) A_{LSZ}^{\text{inst}}(p_2) \overline{A_{LSZ}^{\text{inst}}(-p_1)} \overline{A_{LSZ}^{\text{inst}}(-p_2)}, \end{aligned}$$

$$\mathcal{S}(\chi) \simeq 1 - 6/\chi^4 + 24/\chi^6 + \dots \quad \chi = \frac{R}{\rho} \quad S_{I\bar{I}}(\rho, \bar{\rho}, R) = \frac{4\pi}{\alpha_s(\mu_r)} \mathcal{S}$$

Yung '88
VVK & Ringwald '91
Verbaarschot '91



- Exponential suppression is gradually reduced at lower and lower $\chi = \frac{R}{\rho}$

$$D(\rho, \mu_r) = \kappa \frac{1}{\rho^5} \left(\frac{2\pi}{\alpha_s(\mu_r)} \right)^6 (\rho \mu_r)^{b_0}$$

$$\begin{aligned} \sigma_{\text{tot}}^{(\text{cl}) \text{ inst}} &= \frac{1}{s} \text{Im} \mathcal{A}_4^{I\bar{I}}(p_1, p_2, -p_1, -p_2) \\ &\simeq \frac{1}{s} \text{Im} \int_0^\infty d\rho \int_0^\infty d\bar{\rho} \int d^4 R \int d\Omega D(\rho) D(\bar{\rho}) e^{-S_{I\bar{I}}} \mathcal{K}_{\text{ferm}} \times \\ &\quad A_{LSZ}^{\text{inst}}(p_1) A_{LSZ}^{\text{inst}}(p_2) \overline{A_{LSZ}^{\text{inst}}(-p_1)} \overline{A_{LSZ}^{\text{inst}}(-p_2)}, \end{aligned}$$

fermion prefactor
from Nf qq-bar pairs

$$A_{LSZ}^{\text{inst}}(p_1) A_{LSZ}^{\text{inst}}(p_2) \overline{A_{LSZ}^{\text{inst}}(-p_1)} \overline{A_{LSZ}^{\text{inst}}(-p_2)} = \frac{1}{36} \left(\frac{2\pi^2}{g} \rho^2 \sqrt{s'} \right)^4 e^{iR \cdot (p_1 + p_2)} \exp(-Q(\rho + \bar{\rho}))$$

Q~1GeV formfactor

$$\exp \left(R_0 \sqrt{s} - \frac{4\pi}{\alpha_s(\mu_r)} \hat{\mathcal{S}}(z) \right)$$

But the instanton size has not been stabilised.
In QCD - **rho** is a **classically flat direction** —
need to **include and re-sum quantum corrections!**

in the EW theory:

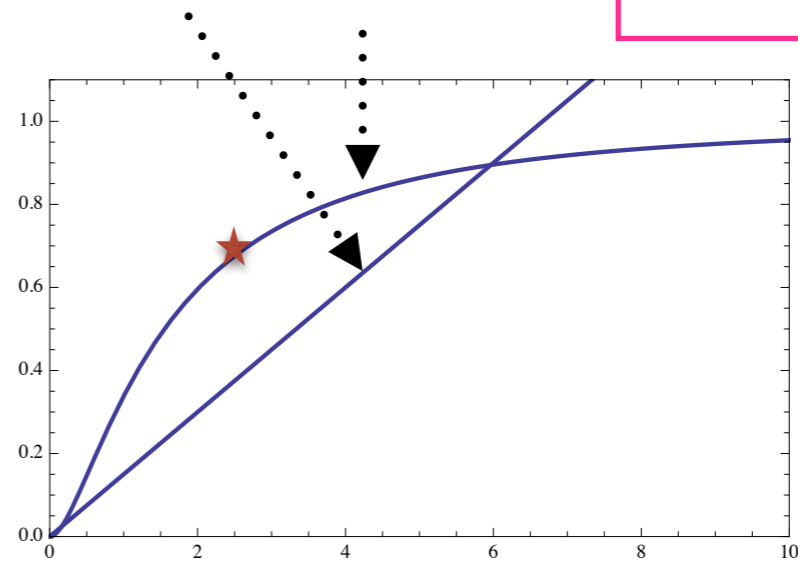
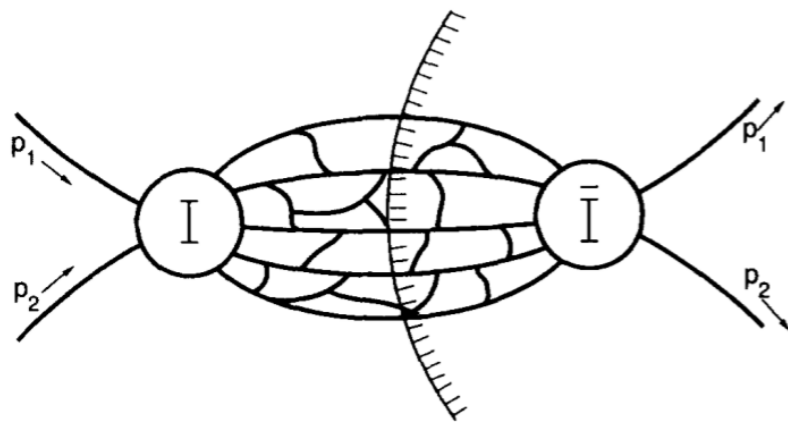
$$G_{4\text{Eucl}} \sim \int d^4 R d\rho_I d\rho_{\bar{I}} \dots \exp \left[i(p_1 + p_2) \cdot R - S_{I\bar{I}}(z) - \pi^2 v^2 (\rho_I^2 + \rho_{\bar{I}}^2) \right]$$

instanton separation
instanton sizes

$$z \sim \frac{R^2 + \rho_I^2 + \rho_{\bar{I}}^2}{\rho_I \rho_{\bar{I}}}$$

Higgs vev:
EW theory - **not QCD!**

$$\sigma_{B+L} \sim \text{Im} \int d^4 R d\rho_I d\rho_{\bar{I}} \dots \exp \left[ER - S_{I\bar{I}}(R) - \pi^2 v^2 (\rho_I^2 + \rho_{\bar{I}}^2) \right]$$



▲
⋮
 Higgs vev cuts-off
 large instantons

- Exponential suppression is gradually reduced with energy [in the EW theory]

In QCD:

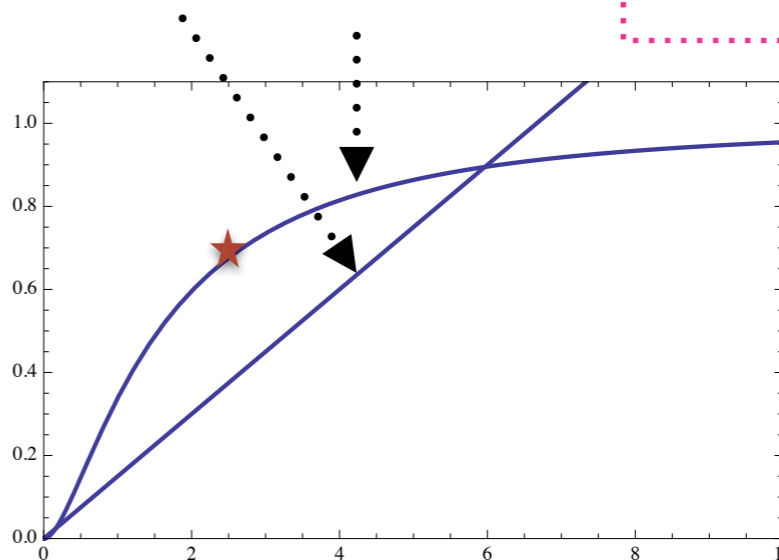
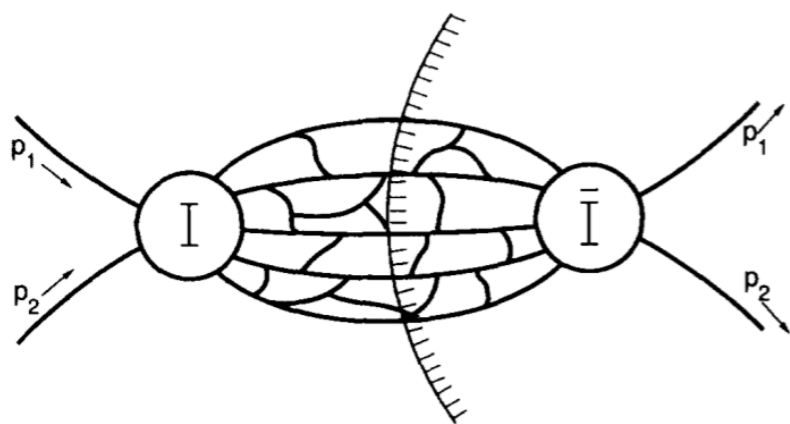
$$G_{4\text{Eucl}} \sim \int d^4 R d\rho_I d\rho_{\bar{I}} \dots \exp [i(p_1 + p_2) \cdot R - S_{I\bar{I}}(z)] \quad \text{- new in QCD}$$

instanton separation
instanton sizes

$$z \sim \frac{R^2 + \rho_I^2 + \rho_{\bar{I}}^2}{\rho_I \rho_{\bar{I}}}$$

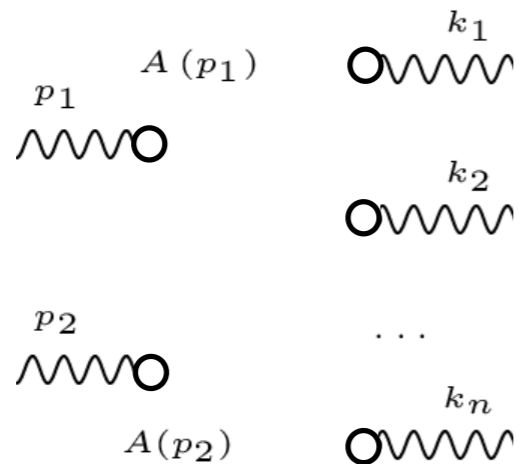
Quantum effects to cut-off Instanton size integrations

$$\sigma_{B+L} \sim \text{Im} \int d^4 R d\rho_I d\rho_{\bar{I}} \dots \exp [ER - S_{I\bar{I}}(R)] \quad \text{- new in QCD}$$



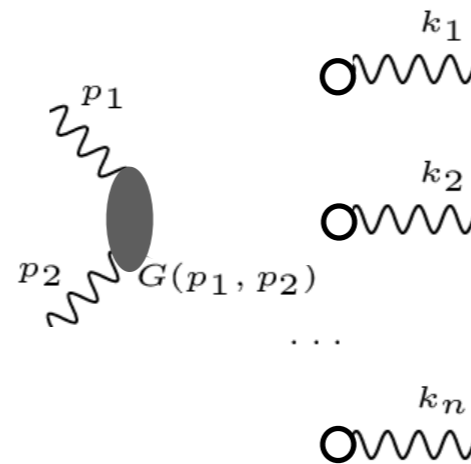
Initial state interactions in the instanton approach

LO instanton process



+

NLO instanton process



propagator in the instanton background

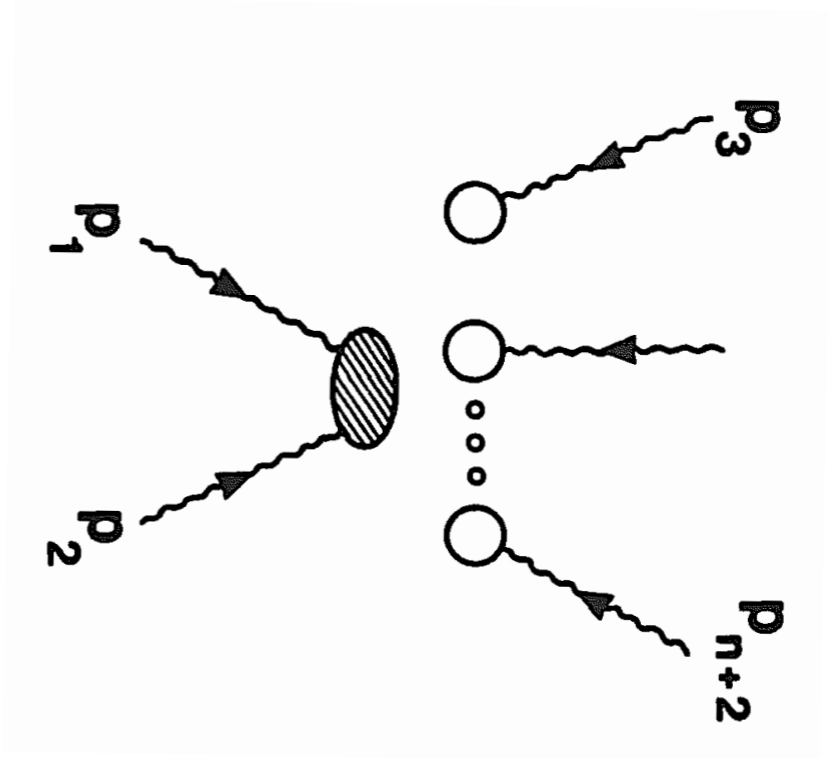
$$G_{\mu\nu}^{ab}(p_1, p_2) \rightarrow -\frac{g^2 \rho^2 s}{64\pi^2} \log(s) A_\mu^a(p_1) A_\nu^b(p_2)$$

$$p_1^2 = 0 = p_2^2, \quad 2p_1 p_2 = s \gg 1/\rho^2$$

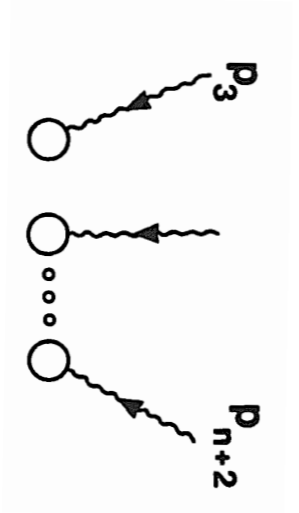
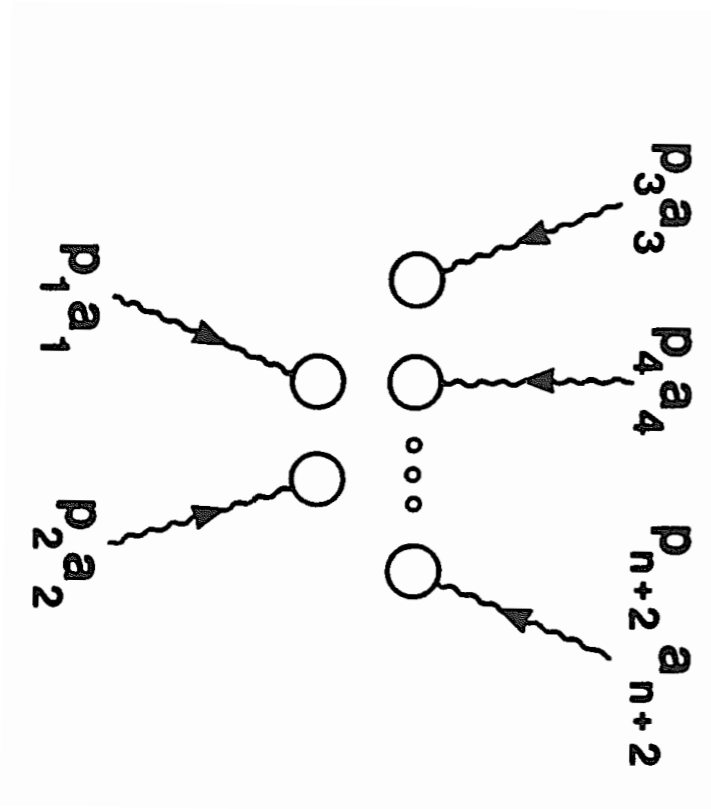
Include now higher order corrections in the high-energy limit:

$$\sum_{r=1}^N \frac{1}{r!} \left(-\frac{g^2 \rho^2 s}{64\pi^2} \log(s) \right)^r A_\mu^a(p_1) A_\nu^b(p_2)$$

Mueller 1991

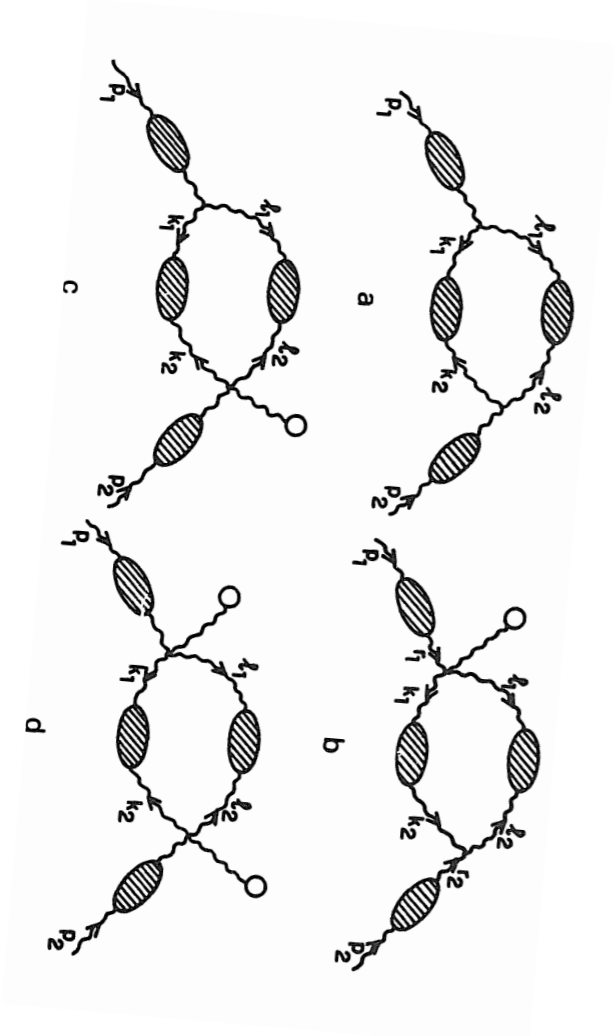


+



+ ...

$$e^{-(\alpha_s(\mu_r)/16\pi) \rho^2 E^2 \log E^2 / \mu_r^2}$$



+

Mueller 1991

Combined effect of initial and final states interactions in QCD

$$\hat{\sigma}_{\text{tot}}^{\text{inst}} \simeq \frac{1}{s'} \text{Im} \frac{\kappa^2 \pi^4}{36 \cdot 4} \int \frac{d\rho}{\rho^5} \int \frac{d\bar{\rho}}{\bar{\rho}^5} \int d^4 R \int d\Omega \left(\frac{2\pi}{\alpha_s(\mu_r)} \right)^{14} (\rho^2 \sqrt{s'})^2 (\bar{\rho}^2 \sqrt{s'})^2 \mathcal{K}_{\text{ferm}} (\rho \mu_r)^{b_0} (\bar{\rho} \mu_r)^{b_0} \exp \left(R_0 \sqrt{s'} - \frac{4\pi}{\alpha_s(\mu_r)} \hat{\mathcal{S}}(z) - \frac{\alpha_s(\mu_r)}{16\pi} (\rho^2 + \bar{\rho}^2) s' \log \left(\frac{s'}{\mu_r^2} \right) \right)$$

Instanton size is cut-off by partonic energy $\sim \sqrt{s}$
 this is what sets the
 effective QCD sphalrenon scale



Quantum corrections
 due to in-in states
 interactions



Basically, in QCD one can never reach the effective sphaleron barrier — it's height grows with the energy.

This is the main idea of the approach:

=> Among other things, no problems with unitarity.

- [1] VVK, Krauss, Schott
- [2] VVK, Milne, Spannowsky

Combined effect of initial and final states interactions in QCD

$$\hat{\sigma}_{\text{tot}}^{\text{inst}} \simeq \frac{1}{s'} \text{Im} \frac{\kappa^2 \pi^4}{36 \cdot 4} \int \frac{d\rho}{\rho^5} \int \frac{d\bar{\rho}}{\bar{\rho}^5} \int d^4 R \int d\Omega \left(\frac{2\pi}{\alpha_s(\mu_r)} \right)^{14} (\rho^2 \sqrt{s'})^2 (\bar{\rho}^2 \sqrt{s'})^2 \mathcal{K}_{\text{ferm}} (\rho \mu_r)^{b_0} (\bar{\rho} \mu_r)^{b_0} \exp \left(R_0 \sqrt{s'} - \frac{4\pi}{\alpha_s(\mu_r)} \hat{\mathcal{S}}(z) - \frac{\alpha_s(\mu_r)}{16\pi} (\rho^2 + \bar{\rho}^2) s' \log \left(\frac{s'}{\mu_r^2} \right) \right)$$

1. Extremise the function in the exponent:
look for a saddle-point in variables:

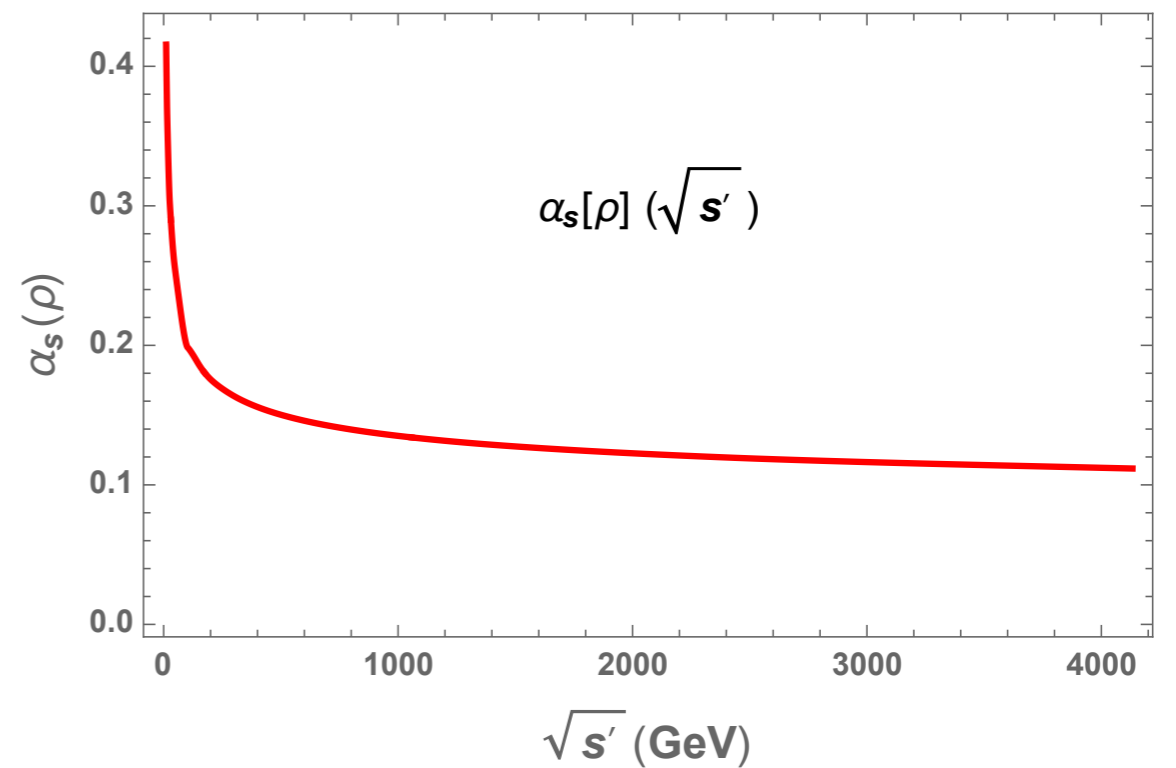
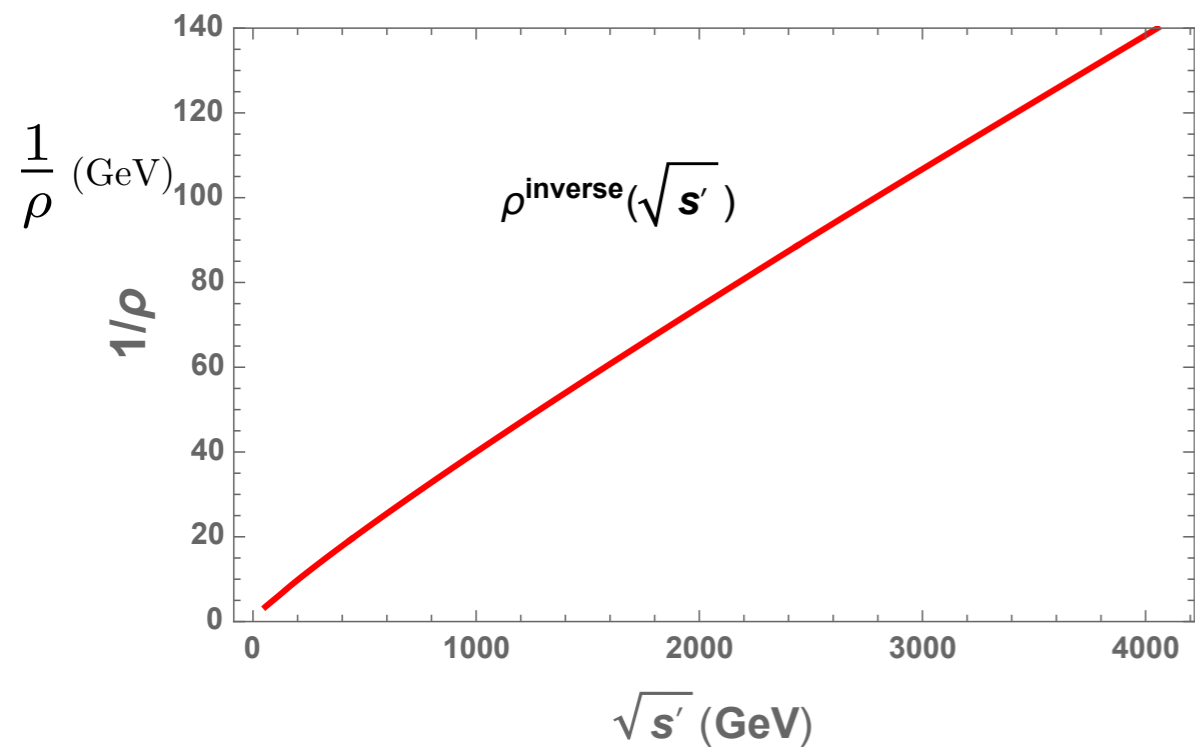
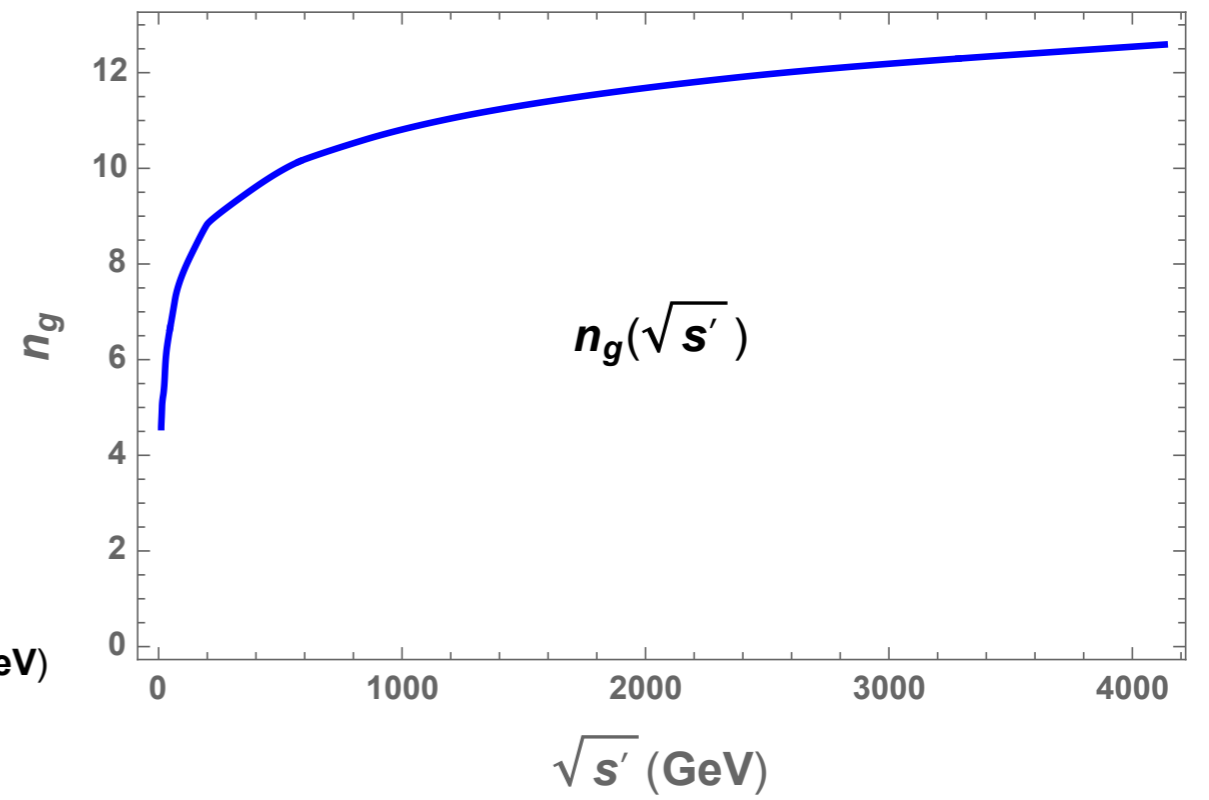
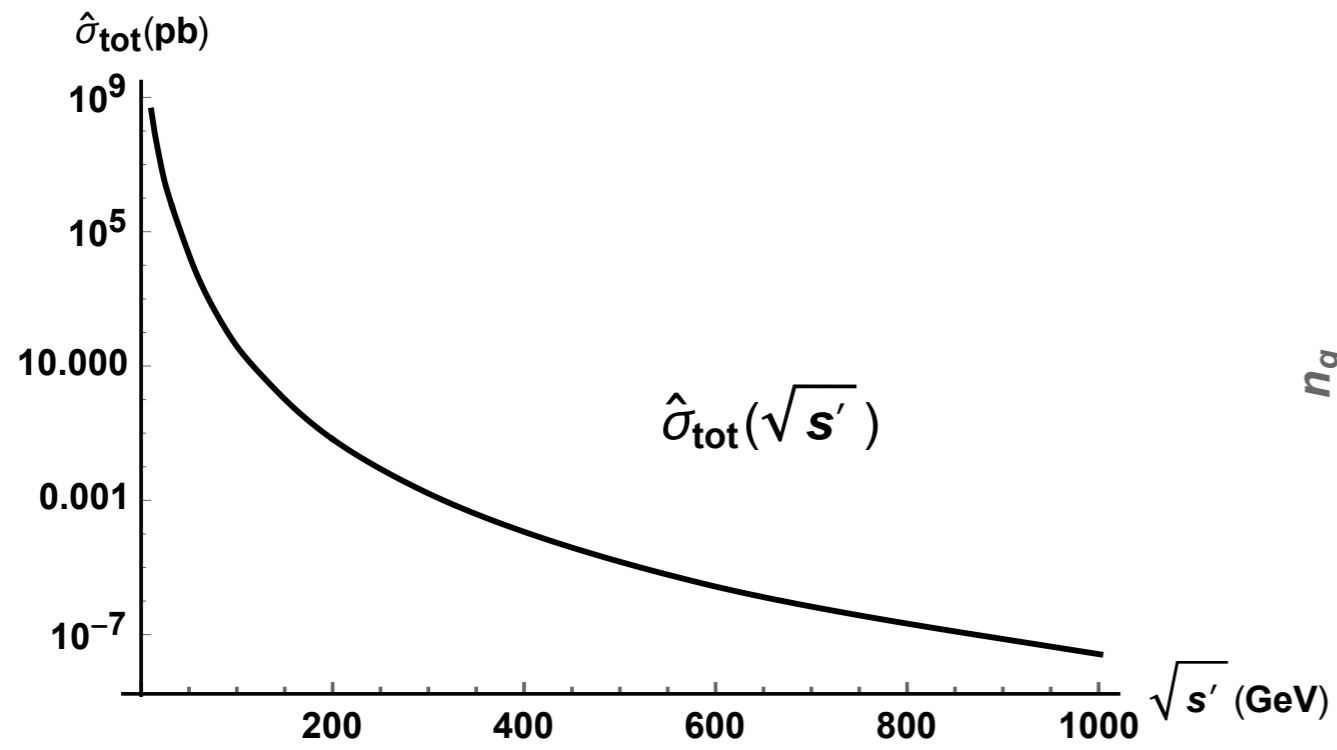
$$\mathcal{F} = \rho \chi \sqrt{s} - \frac{4\pi}{\alpha_s(\rho)} \mathcal{S}(\chi) - \frac{\alpha_s(\rho)}{4\pi} \rho^2 s \log(\sqrt{s} \rho)$$

$$\tilde{\rho} = \frac{\alpha_s(\rho)}{4\pi} \sqrt{s} \rho, \quad \chi = \frac{R}{\rho}$$

- Choice of the RG scale:
 $\mu_r = 1/\langle \rho \rangle = 1/\sqrt{\rho \bar{\rho}}$

2. Carry out all integrations using the steepest descent method evaluating the determinants of quadratic fluctuations around the saddle-point solution
3. Pre-factors are very large — they compete with the semiclassical exponent which is very small!

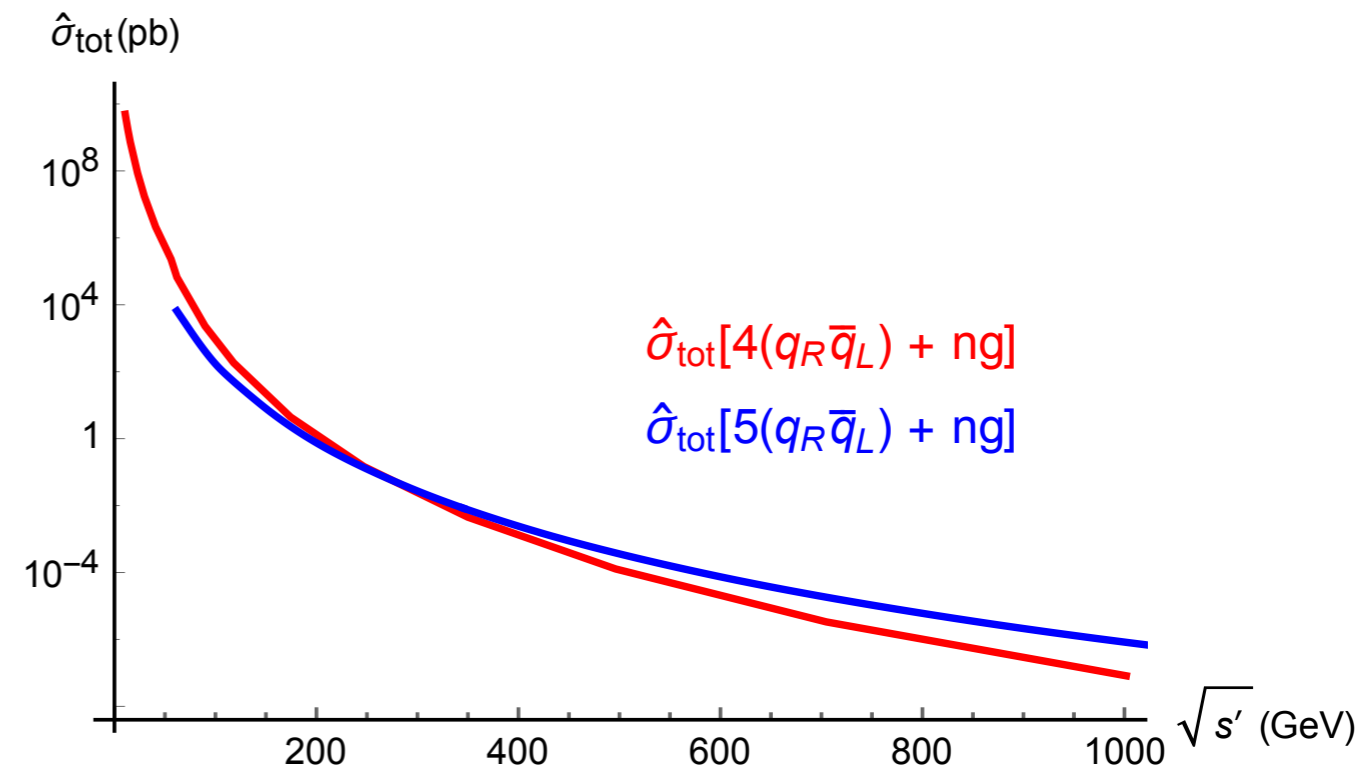
Results



Results for partonic cross-sections

VVK, Krauss, Schott

$\sqrt{s'}$ [GeV]	$1/\rho$ [GeV]	$\alpha_S(1/\rho)$	$\langle n_g \rangle$	$\hat{\sigma}$ [pb]
10.7	0.99	0.416	4.59	$4.922 \cdot 10^9$
11.4	1.04	0.405	4.68	$3.652 \cdot 10^9$
13.4	1.16	0.382	4.90	$1.671 \cdot 10^9$
15.7	1.31	0.360	5.13	$728.9 \cdot 10^6$
22.9	1.76	0.315	5.44	$85.94 \cdot 10^6$
29.7	2.12	0.293	6.02	$17.25 \cdot 10^6$
40.8	2.72	0.267	6.47	$2.121 \cdot 10^6$
56.1	3.50	0.245	6.92	$229.0 \cdot 10^3$
61.8	3.64	0.223	7.28	$72.97 \cdot 10^3$
89.6	4.98	0.206	7.67	$2.733 \cdot 10^3$
118.0	6.21	0.195	8.25	235.4
174.4	8.72	0.180	8.60	6.720
246.9	11.76	0.169	9.04	0.284
349.9	15.90	0.159	9.49	0.012
496.3	21.58	0.150	9.93	$5.112 \cdot 10^{-4}$
704.8	29.37	0.142	10.37	$21.65 \cdot 10^{-6}$
1001.8	40.07	0.135	10.81	$0.9017 \cdot 10^{-6}$
1425.6	54.83	0.128	11.26	$36.45 \cdot 10^{-9}$
2030.6	75.21	0.122	11.70	$1.419 \cdot 10^{-9}$
2895.5	103.4	0.117	12.14	$52.07 \cdot 10^{-12}$



$\sqrt{\hat{s}}$ [GeV]	50	100	150	200	300	400	500
$\langle n_g \rangle$	9.43	11.2	12.22	12.94	13.96	14.68	15.23
$\hat{\sigma}_{\text{tot}}^{\text{inst}}$ [pb]	207.33×10^3	1.29×10^3	53.1	5.21	165.73×10^{-3}	13.65×10^{-3}	1.89×10^{-3}

$$\hat{\sigma}_{\text{tot}}^{\text{inst}}(E) = \frac{1}{E^2} \text{Im} \int_{-\infty}^{+\infty} dr_0 e^{r_0} G(r_0, E),$$

$$\langle n_g \rangle = \langle U_{\text{int}} \rangle$$

$$G(r_0, E) = \frac{\kappa^2 \pi^4}{2^{17}} \sqrt{\frac{\pi}{3}} \int_0^\infty r^2 dr \int_0^\infty \frac{dx}{x} \int_0^\infty \frac{dy}{y} \left(\frac{4\pi}{\alpha_s} \right)^{21/2} \left(\frac{1}{1 - \mathcal{S}(z)} \right)^{7/2} \mathcal{K}_{\text{ferm}}$$

$$r_0 = R_0 E, \quad r = |\vec{R}| E,$$

$$y = \rho \bar{\rho} E^2, \quad x = \rho / \bar{\rho},$$

$$\sum_{n_g=0}^{\infty} \frac{1}{n_g!} (U_{\text{int}})^{n_g} \exp \left(-\frac{4\pi}{\alpha_s} - \frac{\alpha_s}{4\pi} \frac{x + 1/x}{4} y \log y \right).$$

$$\frac{4\pi}{\alpha_s(\langle \rho \rangle)} \simeq \begin{cases} \frac{4\pi}{0.32} - 2b_0 \log(\langle \rho \rangle m_\tau) & : \text{for } \langle \rho \rangle^{-1} \geq 1.45 \text{ GeV} \\ \frac{4\pi}{0.35} & : \text{for } \langle \rho \rangle^{-1} < 1.45 \text{ GeV} \end{cases}$$

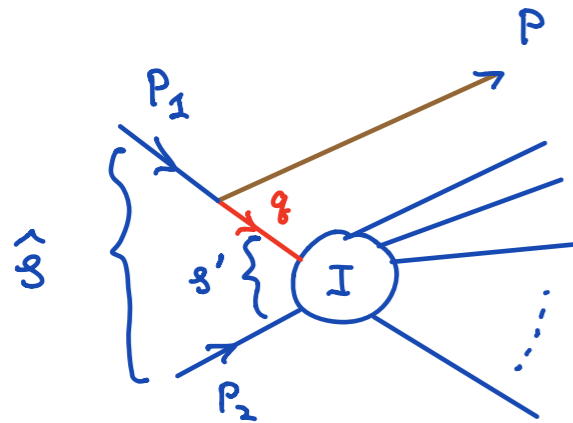
Total hadronic cross-sections for instanton processes are large

$$\sigma_{pp \rightarrow I}(\hat{s} > \hat{s}_{\min}) = \int_{\hat{s}_{\min}}^{s_{pp}} dx_1 dx_2 f(x_1, Q^2) f(x_2, Q^2) \hat{\sigma}(\hat{s} = x_1 x_2 s_{pp})$$

E_{\min} [GeV]	50	100	150	200	300	400	500
$\sigma_{p\bar{p} \rightarrow I}$ $\sqrt{s_{p\bar{p}}} = 1.96$ TeV	2.62 μb	2.61 nb	29.6 pb	1.59 pb	6.94 fb	105 ab	3.06 ab
$\sigma_{pp \rightarrow I}$ $\sqrt{s_{pp}} = 14$ TeV	58.19 μb	129.70 nb	2.769 nb	270.61 pb	3.04 pb	114.04 fb	8.293 fb
$\sigma_{pp \rightarrow I}$ $\sqrt{s_{pp}} = 30$ TeV	211.0 μb	400.9 nb	9.51 nb	1.02 nb	13.3 pb	559.3 fb	46.3 fb
$\sigma_{pp \rightarrow I}$ $\sqrt{s_{pp}} = 100$ TeV	771.0 μb	2.12 μb	48.3 nb	5.65 nb	88.3 pb	4.42 pb	395.0 fb

VVK, Milne, Spannowsky

HOWEVER: If the instanton is recoiled by a high p_T jet emitted from one of the initial state gluons \Rightarrow hadronic cross-section is tiny



$$Q^2 = -q^2 = \sqrt{\hat{s}} p_T$$

$$s' = (q+p_2)^2 = \hat{s} - 2Q^2$$

A virtual leg

$$\Rightarrow e^{-Q^2} \leftarrow \text{form factor.}$$

\uparrow cuts-off

low-energy range.

$$\exp(-Q(\rho + \bar{\rho})) = \exp\left(-\frac{Q}{E} \sqrt{y(x+1/x+2)}\right)$$

Mueller corr.-s

cuts-off high-energy range (as before.)

$\sqrt{\hat{s}}$ [GeV]	310	350	375	400	450	500
$\hat{\sigma}_{\text{tot}}^{\text{inst}}$ [pb]	3.42×10^{-23}	1.35×10^{-18}	1.06×10^{-17}	1.13×10^{-16}	9.23×10^{-16}	3.10×10^{-15}

Table 3. The instanton partonic cross-section recoiled against a hard jet with $p_T = 150$ GeV emitted from an initial state and calculated using Eq. (3.7). Results for the cross-section are shown for a range of partonic C.o.M. energies $\sqrt{\hat{s}}$.

$\sqrt{\hat{s}}$ [GeV]	100	150	200	300	400	500
$\hat{\sigma}_{\text{tot}}^{\text{inst}}$ [pb]	1.68×10^{-7}	1.20×10^{-9}	3.24×10^{-11}	1.84×10^{-13}	4.38×10^{-15}	2.38×10^{-16}

Table 4. The cross-section presented for a range of partonic C.o.M. energies $\sqrt{\hat{s}} = E$ where the recoiled p_T is scaled with the energy, $p_T = \sqrt{\hat{s}}/3$.

Phenomenology

- QCD instanton cross-sections can be very large at hadron colliders.
- Instanton events are isotropic multi-particle final states [in CoM frame]. Event topology is very distinct - can use transverse sphericity & jet broadening event shapes. Also can look for c - \bar{c} pairs in final states.
- Particles with large p_T emitted from the instanton are rare. Especially hard to produce them at low partonic energies (for obvious kinematic reasons). They do not pass high- p_T triggers.
- At large (partonic) energies [$\Rightarrow M_{\text{inst}}$] instanton events can pass high- p_T triggers but have hopelessly suppressed cross-sections.
- Alternative approach 1: Examine data collected with minimum bias trigger [so no high- p_T triggers!]
- Alternative approach 2: + Consider instanton production in diffractive processes looking for final states with large rapidity gaps.

Signal:

The cross-section of instanton production falls steeply with M_{inst} mainly due to the factor $\exp(-S_I) = \exp(-2\pi/\alpha_s(Q))$ in the amplitude.

$$\hat{\sigma}_{\text{inst}} \propto M_{\text{inst}}^{-6} \quad M_{\text{inst}}^{-4}, \text{ at lower energies } 20 - 30 \text{ GeV}$$

Background 1. N-minijets: (high transverse Sphericity final states)

For the perturbatively formed ‘hedgehog’ configuration of N final state jets we would expect

$$\sigma_{\text{pQCD}}(gg \rightarrow N \text{ jets}) \sim \frac{16\pi}{M^2} \left(\frac{N_c}{\pi} \alpha_s(M) \right)^N,$$

where M denotes the invariant energy of the perturbatively formed cluster of minijets. Thus, at sufficiently large values of M_{inst} the instanton signal will become negligible relative to the purely perturbative QCD

=> require $M_{\text{inst}} < 200 \text{ GeV}$ for instantons to dominate

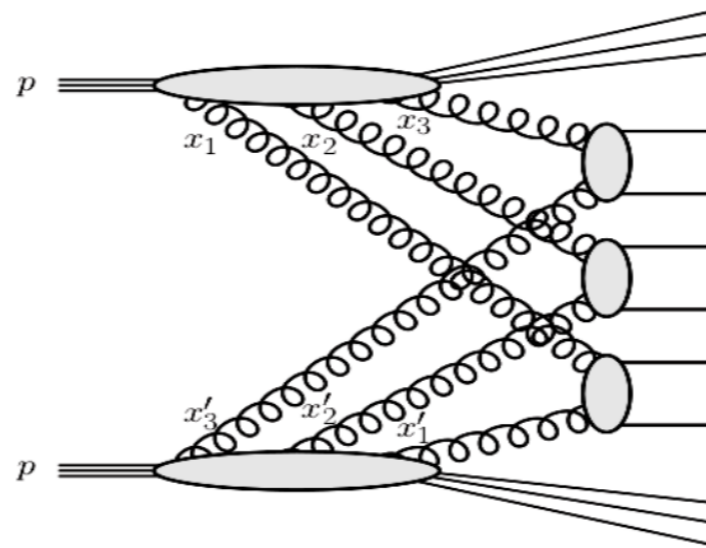
Signal:

The cross-section of instanton production falls steeply with M_{inst} mainly due to the factor $\exp(-S_I) = \exp(-2\pi/\alpha_s(Q))$ in the amplitude.

$$\hat{\sigma}_{\text{inst}} \propto M_{\text{inst}}^{-6} \quad M_{\text{inst}}^{-4}, \text{ at lower energies } 20 - 30 \text{ GeV}$$

Background 2. MPI Multi-parton interactions

MPI backgrounds also have high transverse Sphericicity and dominate over instantons at low $M_{\text{inst}} < 200 \text{ GeV}$



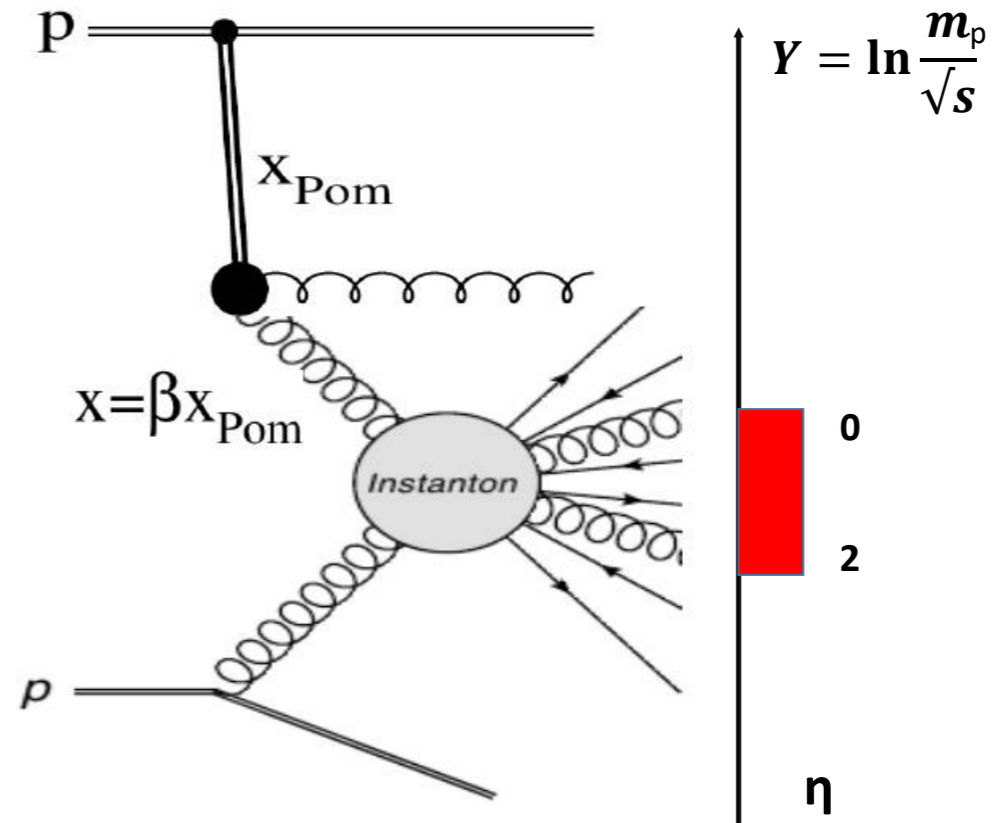
=> would require $M_{\text{inst}} > 200 \text{ GeV}$ for instantons to dominate:
a conundrum!

To suppress MPI and while keeping low-mass $< 200 \text{ GeV}$ instanton contributions use **final state selection with Large Rapidity Gaps**

Instanton cross-sections are large, but one needs to be creative in separating instanton signal from large QCD background.

One such strategy is search for QCD instantons in diffractive events at the LHC: QCD background caused by multi-parton interactions can be effectively suppressed by selecting events with large rapidity gaps

$$\sum_i E_{T,i} > 30 \text{ GeV}, N_{ch} > 25$$



use multi-jet cuts

use low luminosity runs to avoid problems with large pile-up

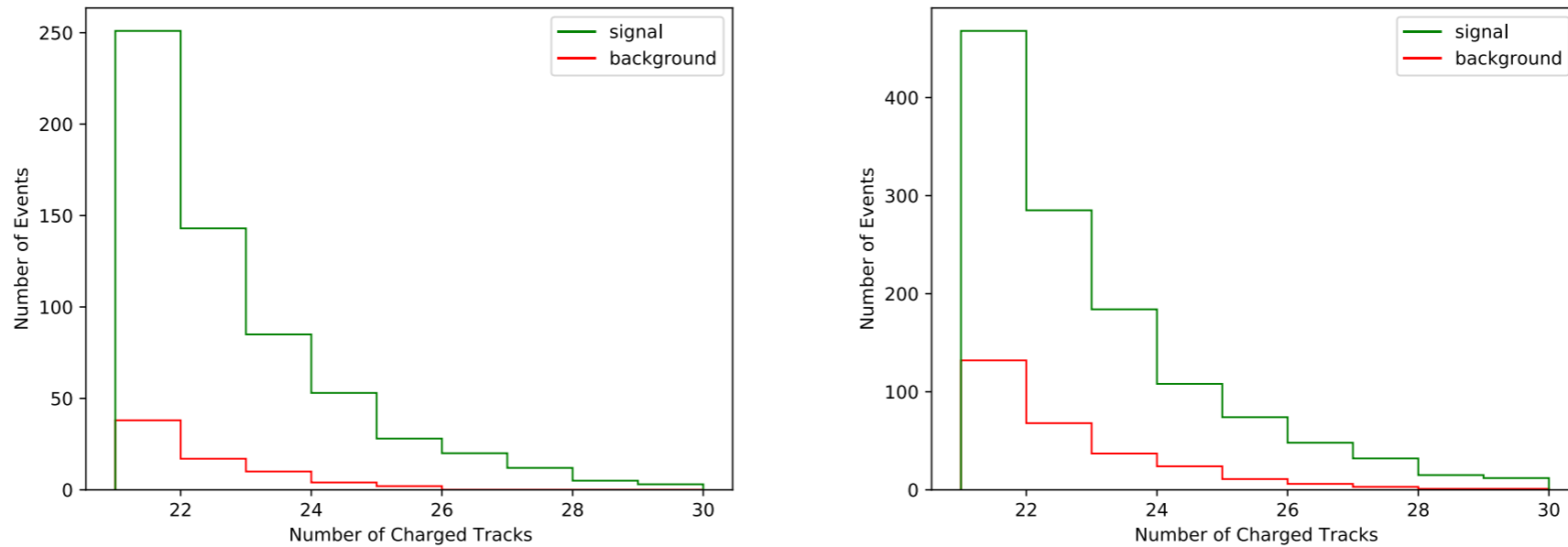


Figure 3: Multiplicity distribution of charged hadrons produced in the events with the instanton (green) in comparison with the expected background (red).

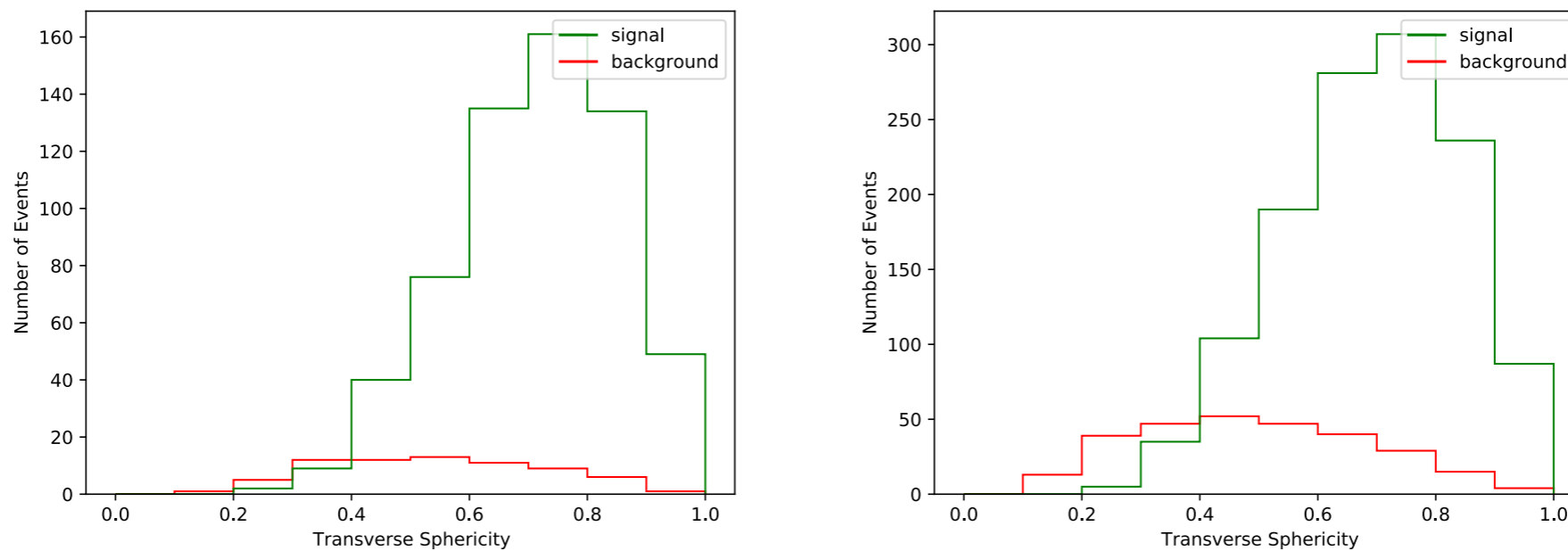
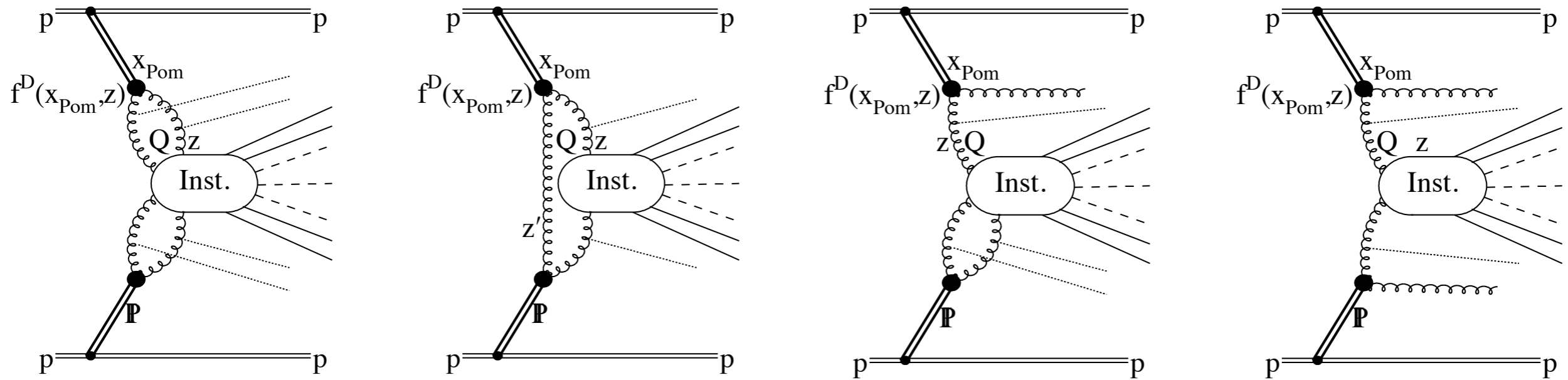


Figure 4: Distribution over the transverse sphericity S_T , Eq. (8), of the charged hadrons produced in the events with the instanton (green) in comparison with the expected background (red).

We have also considered central instanton production in diffractive events with two rapidity gaps:



Latest theoretical results look promising. More detailed phenomenological and ultimately experimental studies are needed and will hopefully follow.

VA Khoze, VVK, Dan Milne, Misha Ryskin: 2111.02159

General lesson: to see instantons at colliders - need to be inventive with experimental strategies!

[Extra slide] Theoretical uncertainties

- QCD Instanton rates are interesting in the regime where they become large — lower end of partonic energies 20-80 GeV. The weak coupling approximation used in the semiclassical calculation can be problematic.
- What is the role of higher-order corrections to the Mueller's term in the exponent?
- Possible corrections to the instanton-anti-instanton interaction at medium instanton separations in the optical theorem approach.
- Non-factorisation of the determinants in the instanton-anti-instanton background in the optical theorem. (Instanton densities $D(\rho)$ do not factorise at finite $R/\rho \sim 1.5 - 2$.)
- Choice of the RG scale = $1/\rho$. (can vary by a factor of 2 or use other prescriptions to test. In Ref. [1] we checked that)
- A practical point for future progress is to test theory normalisation of predicted QCD instanton rates with data. [The unbiased un-tuned theory prediction looks promising.]